ADA075507

...RISON OF ABLATIVE MATERIALS
...LID ROCKET MOTOR FLOW FIELD

...Department

NAVAL SURFACE WEAPONS CENTER

Dahlgren, Virginia 22448 ... Silver Spring, Ma...

NAVAL SURFACE WEAPONS CENTER
Dahlgren, Virginia 22448

[illegible] Anderson, Capt. USN
Commander

UNCLASSIFIED
SECURITY CLASSIFICATION OF THIS PAGE (When Data Entered)

REPORT DOCUMENTATION PAGE

READ INSTRUCTIONS BEFORE COMPLETING FORM

1. REPORT NUMBER: NSWC TR 79-218	2. GOVT ACCESSION NO.
3. RECIPIENT'S CATALOG NUMBER	
4. TITLE (and Subtitle): COMPARISON OF ABLATIVE MATERIALS IN A SOLID ROCKET MOTOR FLOW FIELD	5. TYPE OF REPORT & PERIOD COVERED: Final, Sep 78 - Jan 79
	6. PERFORMING ORG. REPORT NUMBER
7. AUTHOR(s): J. Henderson, L. Anderson, G. Moore	8. CONTRACT OR GRANT NUMBER(s)
9. PERFORMING ORGANIZATION NAME AND ADDRESS: Naval Surface Weapons Center (N43), Dahlgren, VA 22448	10. PROGRAM ELEMENT, PROJECT, TASK AREA & WORK UNIT NUMBERS: 62332N:F32392:SF32392: 9N76FA500
11. CONTROLLING OFFICE NAME AND ADDRESS: Naval Sea Systems Command, Washington, DC 20362	12. REPORT DATE: August 1979
	13. NUMBER OF PAGES: 40
14. MONITORING AGENCY NAME & ADDRESS (if different from Controlling Office)	15. SECURITY CLASS. (of this report): UNCLASSIFIED
	15a. DECLASSIFICATION/DOWNGRADING SCHEDULE

16. DISTRIBUTION STATEMENT (of this Report)

Approved for public release; distribution unlimited.

17. DISTRIBUTION STATEMENT (of the abstract entered in Block 20, if different from Report)

18. SUPPLEMENTARY NOTES

19. KEY WORDS (Continue on reverse side if necessary and identify by block number)

ablative materials	FR-1	rocket motors
Haveg 41	Fondu-Fyre WA-1	TOMAHAWK
Haveg 41N	HDFG Carbon	erosion depth
MXB-360	MXBE-350	temperature profiles

20. ABSTRACT (Continue on reverse side if necessary and identify by block number)

Seven different ablative materials have been tested behind Thiokol TOMAHAWK rocket motors. The maximum erosion, erosion patterns, and the mass loss of the samples have been determined from these tests. In addition, time-dependent temperature profiles were measured in four of the test samples during firing. From these data, local ablation rates for the materials were determined.

DD FORM 1 JAN 73 1473 EDITION OF 1 NOV 65 IS OBSOLETE
S/N 0102-LF-014-6601

UNCLASSIFIED
SECURITY CLASSIFICATION OF THIS PAGE (When Data Entered)

FOREWORD

This work was performed as part of the investigation to determine methods of protecting shipboard structures from the damaging effects of missile exhausts. Funding for this general task area was provided by Naval Sea Systems Command, SEA 035.

This study was performed in conjunction with ongoing NASA, Huntsville, Alabama, scale-model space-shuttle tests. The Naval Surface Weapons Center was invited to participate in these tests at no cost. The cooperation of NASA personnel was consistently outstanding. The authors would like to express their appreciation for the support of NASA's instrumentation and test groups, without whose help this work could not have been accomplished.

This work was reviewed and approved by J. J. Yagla, Head, Ship Safety Engineering Branch, and P. D. Malcolm, Head, Systems Safety Division.

Released by:

G. O. MILLER, Head
Combat Systems Department

CONTENTS

SI Conversion

Multiply	By	To Obtain
inch (in.)	2.540	centimeter (cm)
degree Fahrenheit (°F)	(after subtracting 32) 0.5556	degree Celsius (°C)
pound (lb)	0.4536	kilogram (kg)
pound-force (lbf)	4.4482	newton (N)
pound-force/inch^2 atmosphere (psia)	6894	pascal (Pa)

INTRODUCTION

Tests were recently performed at Naval Aeronautics and Space Administration's (NASA) Marshall Space Flight Center, Huntsville, Alabama, to determine the performance of seven types of candidate protective/ablative materials. The ablative, erosive, and thermal responses of these materials were examined. These properties are important in the selection of materials to protect a region where direct impingement from rocket motors during restrained or normal firings are of concern. Because of the variable conditions under which ablative materials must perform, no single type of material is well suited for all applications. Certain areas, such as launchers or areas over fuel tanks, require highly insulative materials. Deck areas may require less thermal protection, but because of heavy traffic may need a durable material. In addition, the type of motor and the geometry of the plenum, deck, bulkhead, etc., govern the thickness and dimensions of the material to be used.

Most ablative-material testing done by the Navy has been performed as needed and has been directed towards a special application. This method of testing provides the basic information required to solve the specific problem but does little to provide data that can be extrapolated to fit varied classes of problems. This work is an initial effort to screen and classify candidate ablative materials for general use and to create a broad base of experimental data that can be applied to a large category of applications.

DESCRIPTION OF TESTS

GENERAL

Five tests were conducted using two different test plenums. Each test utilized two Thiokol TOMAHAWK motors*, designated L and R, to simulate, at reduced scale, the launch of the space-shuttle vehicle. One ablative material sample was placed under each rocket motor. The distance and angle of the samples with respect to the rocket motors were different in each plenum. These dimensions are depicted in Figures 1 and 2. The two plenum configurations are shown in Figures 3 and 4.

MATERIALS

Ten samples consisting of seven different ablative materials were tested between December 1978 and April 1979. These materials were generally classified

---

* The Thiokol version of the TOMAHAWK motor was not selected in competition for TOMAHAWK production missiles. Hence, the data in this report do not apply to developmental or production TOMAHAWK missiles. Motor data are provided in Appendix A.

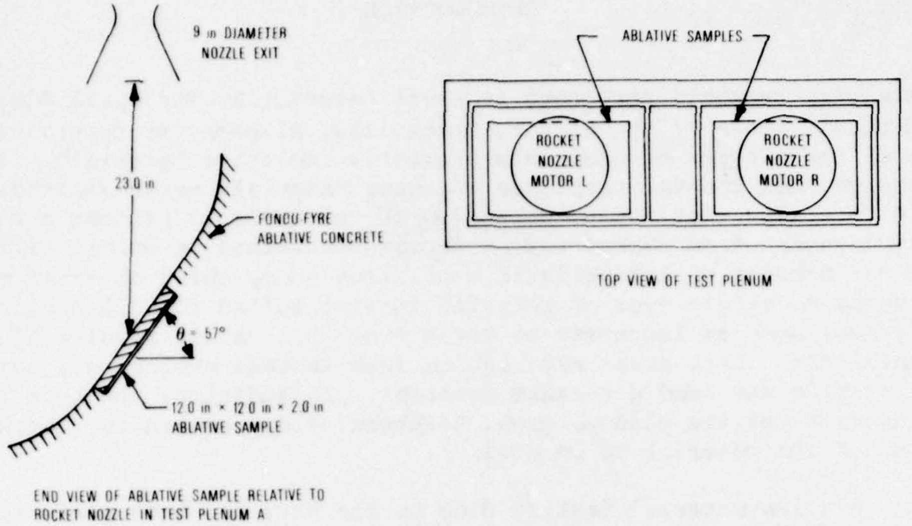

Figure 1. Location of Ablative Sample with Respect to Motors in Plenum Configuration A

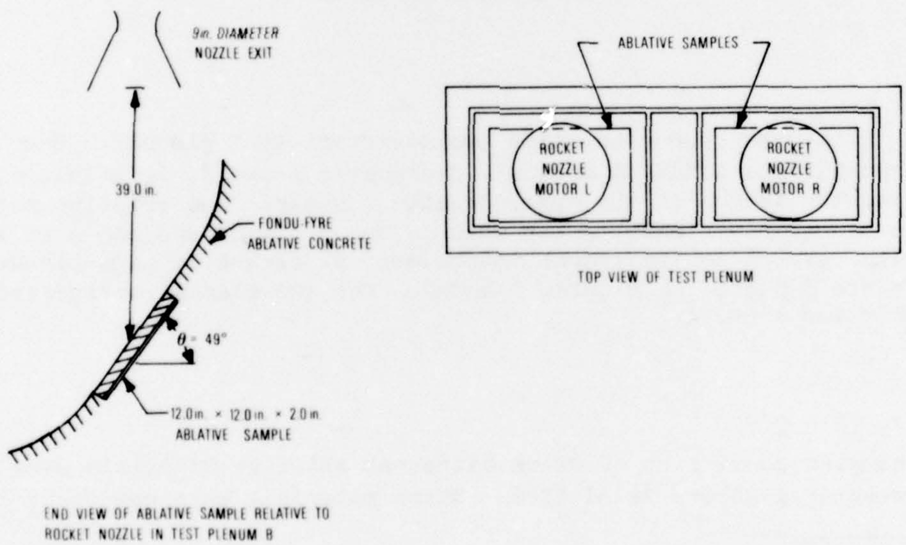

Figure 2. Location of Ablative Sample with Respect to Motors in Plenum Configuration B

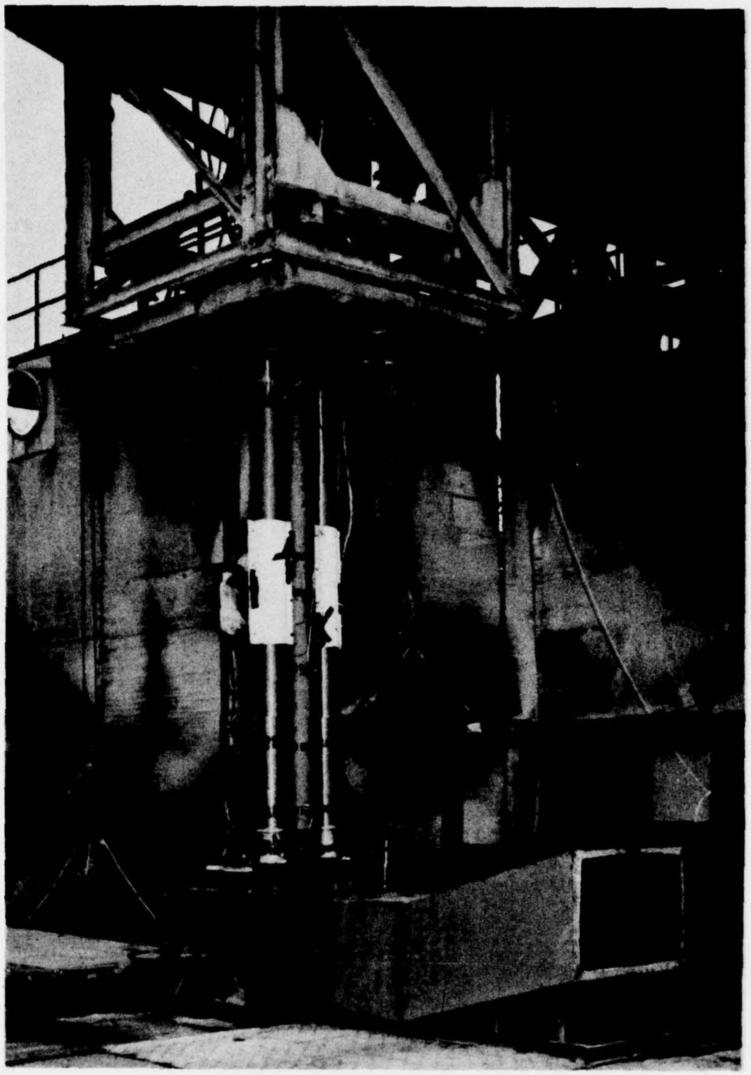

Figure 3. Test Plenum A

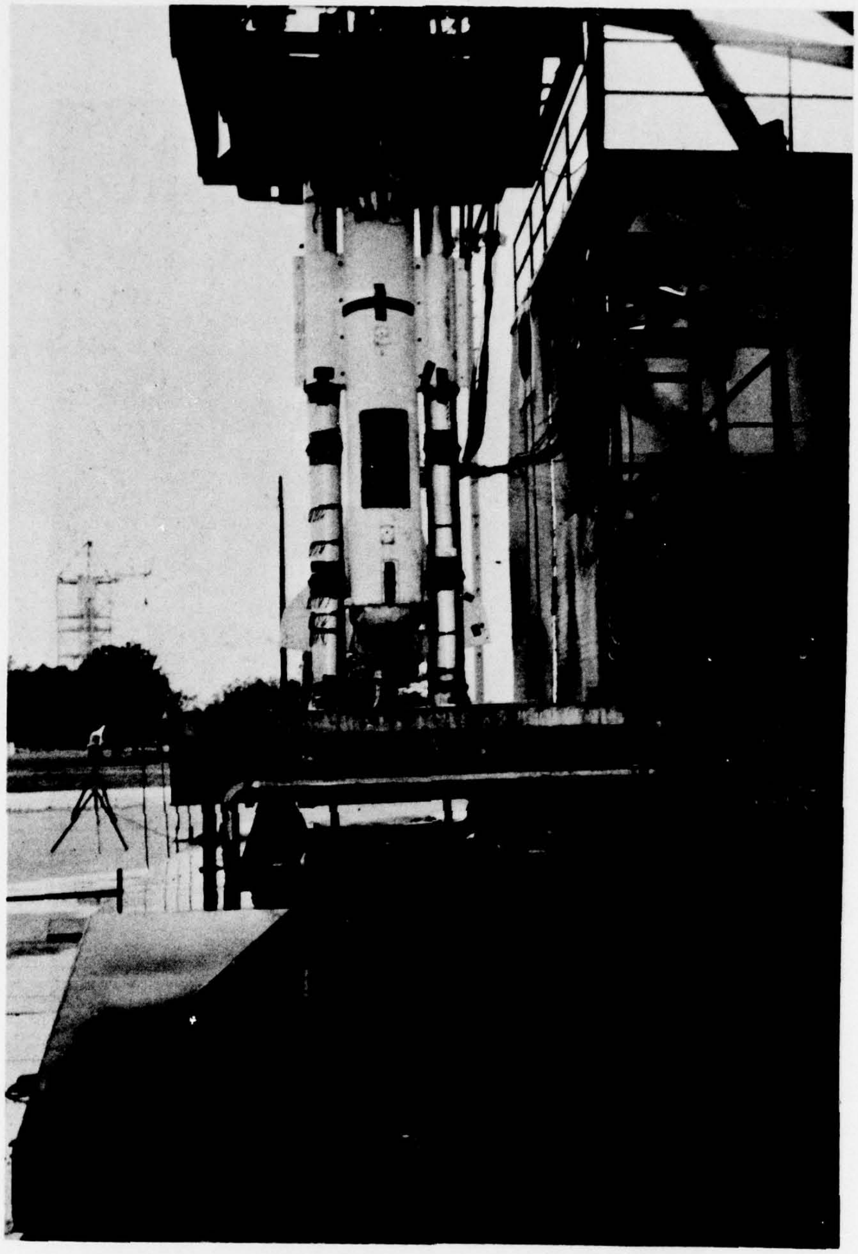

Figure 4. Test Plenum B

into three categories: low thermal conductivity charring ablators, low thermal conductivity melting ablators, and high thermal conductivity subliming ablators. As shown in Table 1, the majority of the materials tested were the charring ablator types. Several of these materials have been tested many times in the past and have been shown to be good thermal protection materials. The Haveg materials and Fiberite MXB-360 are excellent thermal protection materials and are being used or being considered for use for naval shipboard applications. The Fiber Materials (FR-1) and HDFG are relatively new and have not previously been tested. The Fondu-Fyre WA-1 is an ablative concrete that has been used by NASA for many years but has not been considered for naval applications.

PROCEDURE

The material samples were cut and machined to 12 x 12 x 2 in., with a 0.5- x 0.5-in. groove around the top edge. After machining, the samples were weighed and gauged to ensure that the proper dimensions had been obtained. The samples were then bonded to 15- x 15- x 0.125-in. steel plates and bolted in the plenum. In order to provide additional support, a mixture of Fondu-Fyre ablative concrete was placed around each sample. Figure 5 shows the samples placed in plenum B before testing.

Table 1. Summary of Materials Tested

Ablative Material	Composition	Manufacturer	Thermal Characteristics	Type of Ablator
41	Asbestos Phenolic	Haveg	Insulator	Charring
41N	Silica Phenolic	Haveg	Insulator	Charring
MXB-360	Glass Phenolic	Fiberite	Insulator	Charring
MXBE-350	Rubber-Modified Glass Phenolic	Fiberite	Insulator	Charring
Fire Retardant (FR-1)	Silica and Organic Resin	Fiber Materials	Insulator	Charring
Fondu-Fyre WA-1	Ablative Concrete	Designed Concretes	Insulator	Melting
HDFG Carbon	Carbon-Carbon	Fiber Materials	Conductor	Subliming

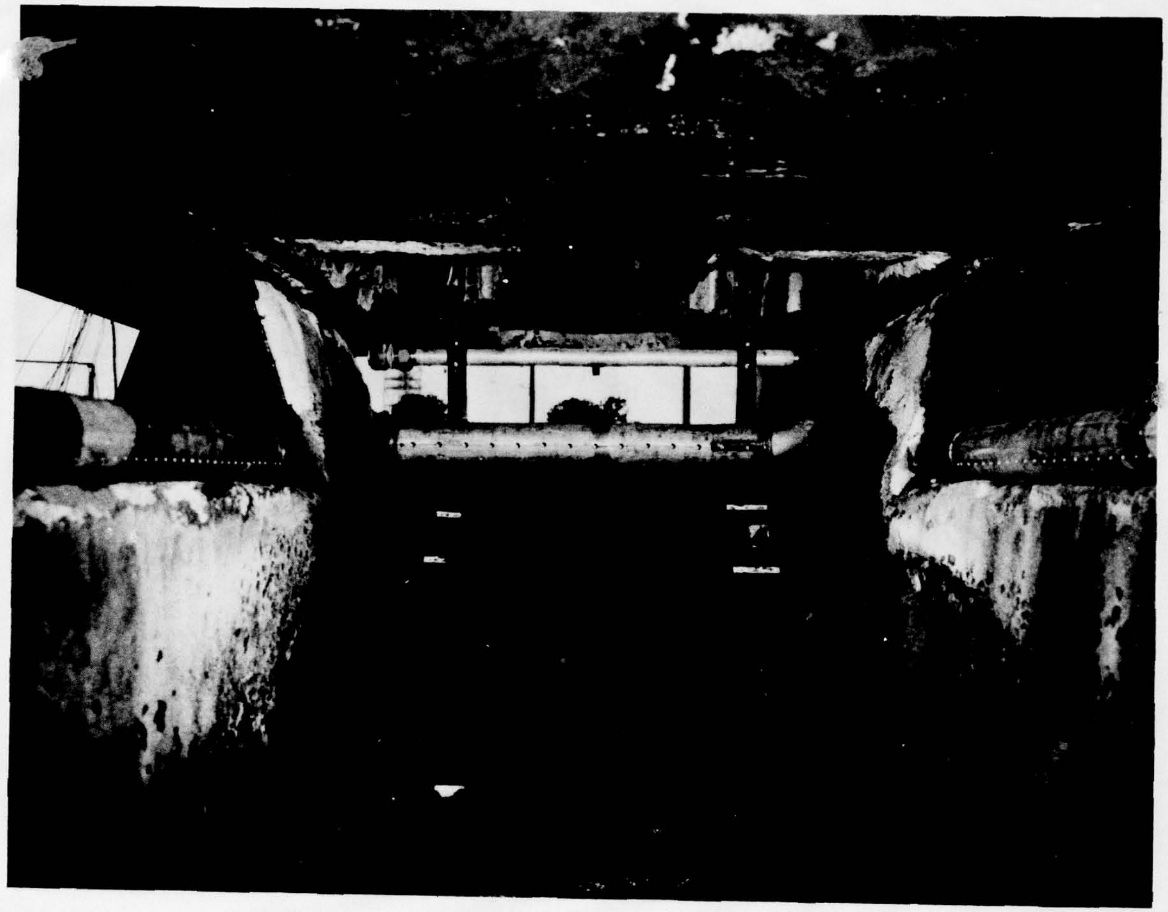

Figure 5. Ablative Samples in Test Plenum B

Thermocouples were placed in the last four samples tested. Four 0.125-in. diameter holes were drilled in the back of each sample, and a 30-gauge chromel-alumel thermocouple was placed in each hole in addition to one on the top surface and one on the bottom surface of the samples. In order to minimize errors, the holes were filled with materials whose thermal properties matched those of the original material as closely as possible. The approximate depths, location of the holes, and the dimensions of the samples are depicted in Figure 6.

After testing, the samples and all excess bonding material were removed from the steel plate. The samples were then weighed and gauged on 1-in. grids to obtain maximum erosion depth and the data points necessary to draw erosion contours. The average surface regression was estimated by placing the samples in a calibrated water tank and measuring the total water displacement.

In addition to the temperature measurements made in the last four samples, the chamber pressure was measured in each rocket motor during firing. Both the pressure and thermocouple data were digitized at 40-ms intervals by NASA's instrumentation group.

RESULTS

The experimental maximum erosion depths and total mass losses for each test material are summarized in Table 2. Tests 1 and 2 were conducted in plenum configuration A, while tests 3, 4, and 5 were conducted in plenum B. The two motors used in each test are designated L and R. A comparison of the maximum erosion depths and total mass losses of either Haveg 41 or 41N, which were tested several times, shows that there was significant variation in the erosion of these materials between plenum configurations A and B. This was expected since the distance from the nozzle exit to the ablative sample, the angle of the sample relative to the motor axis, and the side wall locations varied between the two plenum configurations (see Figures 1 and 2). There was also significant variation in maximum erosion depths and total mass losses between motors in the same plenum. Upon examination of the plenum side walls, it was found that the exhaust plume interacted with the side walls. Furthermore, the side walls on either side of motors L and R were not identical in shape, thus causing a variation in the exhaust flow between each motor.

The fact that Haveg 41 and Haveg 41N were tested several times allows indirect comparisons to be made between all of the samples. These comparisons are made easier by grouping the samples according to plenum and rocket motor location as shown in Table 3. This table shows maximum erosion depth, percentage mass loss, and the average surface regression for each material within the four possible groups. The side walls of the plenums were refurbished between each test; thus only small variations occurred within the same plenum between firings. Comparisons can be made between each of the groups and thus a comparison of the individual ablative materials. In addition, rocket motor chamber pressure data were taken during each test and are shown in Appendix B. There was very little variation in chamber pressure between motors.

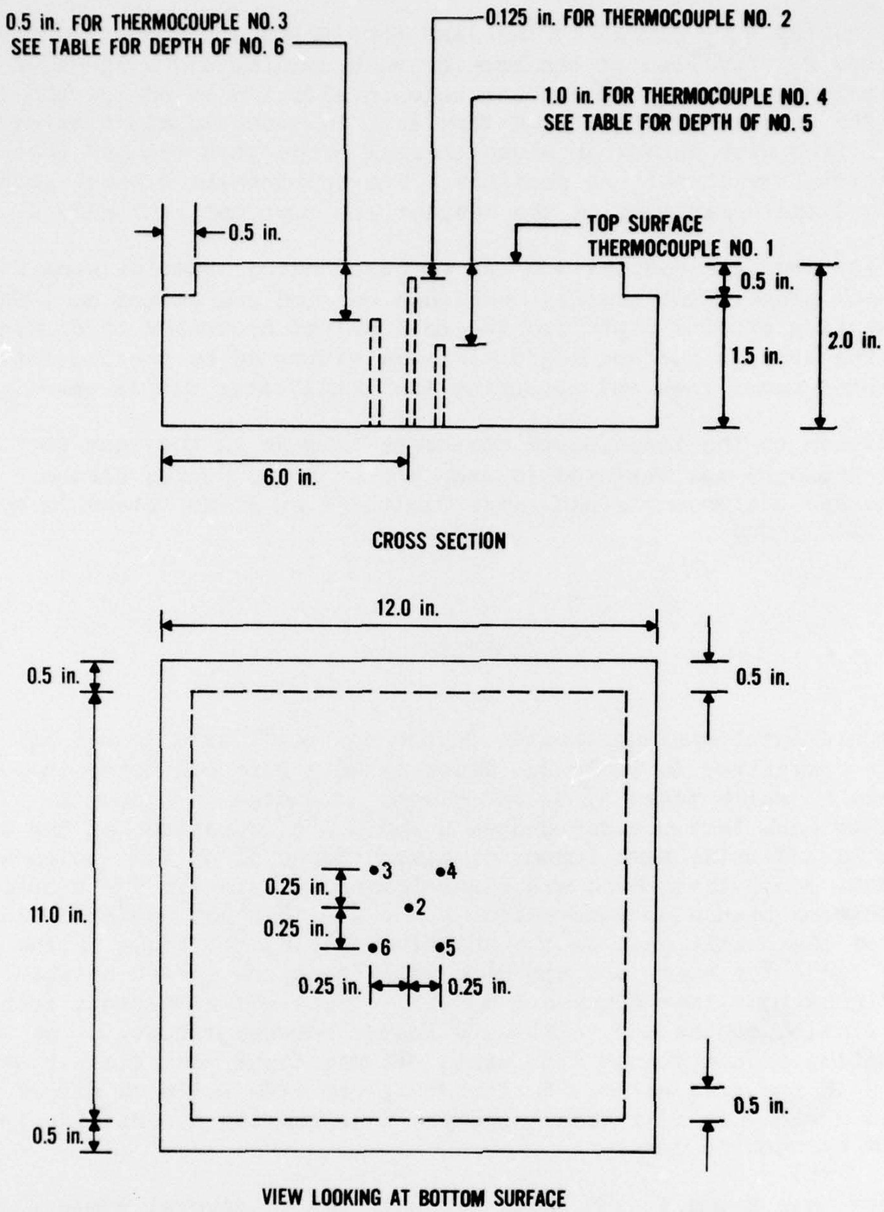

THERMOCOUPLE NO.	DEPTH FROM TOP SURFACE (in.)
1	0.000
2	0.125
3	0.50
4	1.00
5	1.50
6	2.00

Figure 6. Sample Dimensions and Thermocouple Locations

Table 2. Summary of Huntsville Test Data

Plenum Configuration	Test and Date	Motor	Ablative Material	Dimension (in.)	Virgin Density (lbm/ft^3)	Maximum Erosion Depth (in.)	Weight (lbm) Before Firing	Weight (lbm) After Firing	Loss Mass (lbm)	Loss Weight (%)
A	1 12/08/78	L	41	12 x 12 x 2	105.0*	0.879	16.84*	14.16	2.68*	16.0*
		R	41N	12 x 12 x 2	122.0*	0.927	19.60*	16.32	3.28*	16.7*
	2 12/15/79	L	MXB-360	12 x 12 x 2	113.28*	0.807	18.88*	15.70	3.18*	16.8*
		R	Fire Retardant (FR-1)	12 x 12 x 2	94.21*	0.880	15.70*	10.01	5.69*	36.2*
B	3 03/08/79	L	41N	12 x 12 x 2	122.0*	1.399	19.60	14.80	4.80	24.5
		R	41	12 x 12 x 2	105.0*	1.122	16.84	12.93	3.91	23.2
	4 03/28/79	L	Fondu-Fyre WA-1	12 x 12 x 2.045	127.16	1.435	20.78	14.78	6.00	28.9
		R	41N	12 x 12 x 2	116.06	1.122	18.57	14.55	4.02	21.6
	5 04/17/79	L	HDFG Carbon	12 x 12 x 1.784	98.20	0.425	13.91	12.80	1.11	8.0
		R	MXBE-350	12 x 12 x 2	106.93	1.323	17.11	12.69	4.42	25.8

Approximate values

Table 3. Huntsville Data Grouped by Plenum and Motor

Plenum Configuration	Motor	Group	Test	Ablative Material	Maximum Erosion Depth (in.)	Average Surface Regression (in.)	Mass Loss (%)
A	L	1	1	41	0.879	0.356	16.0
			2	MXB-360	0.807	0.397	16.8
	R	2	1	41N	0.927	0.356	16.7
			2	Fire Retardant (FR-1)	0.880	0.484	36.2
B	L	3	3	41N	1.399	---	24.5
			4	Fondu-Fyre WA-1	1.435	0.768	28.9
			5	HDFG Carbon	0.425	0.230	8.0
	R	4	3	41	1.122	0.524	23.2
			4	41N	1.122	0.548	21.6
			5	MXBE-350	1.323	0.584	25.8

Furthermore, if it is assumed that the relative performance of each of the materials tested is independent of the test conditions (impingement distance, angle, etc.), then a comparison of all of the materials can be made. For example, Haveg 41 and 41N have the same maximum erosion depth for plenum configuration B, motor R (group 4); therefore, their maximum erosion depth would be the equal if they were both tested in plenum A, motor L, etc. With this assumption and the fact that 41 and 41N were both tested in group 4, the performance of all of the ablative materials can be determined relative to either 41 or 41N. Table 4 shows the relative erosion performance of each of the materials tested. The results have been normalized with respect to the performance of Haveg 41N and are based both on maximum erosion depth and total mass loss. The larger the value of the ablative material's performance index, the less the material ablated. Based on maximum erosion depth, the performance of the melting and charring ablators is within 10 to 15 percent of that for Haveg 41N. Because of the uncertainty in the rocket motor exhaust environment, these differences are probably not significant.

Table 4. Relative Performance of Ablative Materials Based on Maximum Erosion Depth and on Total Mass Loss

Ablative Material	Relative Performance: Maximum Erosion	Relative Performance: Total Mass Loss
HDFG Carbon	3.29	3.06
MXB-360	1.09	0.89
Fire Retardant (FR-1)	1.05	0.46
41N	1.00	1.00
41	1.00	0.93
Fondu-Fyre WA-1	0.97	0.85
MXBE-350	0.85	0.84

As shown in Table 4, the subliming ablator, HDFG carbon, erodes considerably less than the other types of ablators and is approximately three times better than Haveg 41N.

The performance of the ablative materials based on total mass loss in general follows the same trends as that based on maximum erosion depth. An exception is the Fiber Material (FR-1) ablative. This material has a very high total mass loss (relative performance 0.46), while its maximum erosion depth (relative performance 1.05) is better than that of Haveg 41N. This is caused by a more even erosion pattern and partial decomposition of the FR-1.

This phenomenon can be explained by examining the average surface regression (total volume of material lost divided by the surface area) for the materials. Using the average surface regression, the total mass loss can be computed based on the virgin material density. For FR-1, the measured total mass loss was 5.69 lb; the computed mass loss based on the average surface regression is 3.80 lb. This indicates that the remaining FR-1 material must have undergone partial pyrolysis causing a decrease in density in some of the remaining material. All of the other materials showed good agreement between the measured total mass loss and the computed value based on the average surface regression.

Erosion patterns for each sample were generated by a general-purpose CalComp* contouring program using either 121 or 132 grid points. The results of the calculations are shown in Figures 7 through 16. These figures are oriented as they were in the plenum; i.e., top edge of the contour was nearest the nozzle exit. Note that maximum depths in general occur on the side of the sample nearest to the plenum side wall.

The temperature profiles for the last four samples tested are shown in Figures 17 and 18. Only the profiles for the 0.125- and 0.50-in. depths are shown in Figure 17. The exact depths of the thermocouples are shown on their respective plots. Both materials in Figure 17 are excellent insulators; therefore, the temperature rise precedes the pyrolysis interface by only very small times. Figure 18 depicts the results of the last tests in which one insulative material, MXBE-350, and one high thermal conductivity material, HDFG carbon, were tested. The results for the MXBE-350 curve are similar to those in Figure 17; however, the HDFG carbon material exhibits a much different behavior. Because of the high thermal conductivity of the HDFG, the heat is diffused through the material at a much higher rate; therefore, temperature curves from four in-depth thermocouples are plotted in order to show the temperature distribution in the material.

Average local ablative rates were obtained for plenum configuration B by dividing the distance (ΔX) between the in-depth thermocouples by the time (Δt) required for the point to reach the given temperature. This was done for Fondu-Fyre WA-1, Haveg 41N, and MXBE-350. Since the temperature rise in these materials occurs over a very short time (good thermal insulators), this value is very near the material ablation rate. The HDFG did not ablate sufficiently to reach the first thermocouple and the time rise time is a function of the depth at the thermocouple; therefore, no ablation rate could be calculated. The ablative rates between the first and second thermocouple for MXBE-350 and 41N were approximately the same (0.071 in./sec) whereas the corresponding ablative rate for WA-1 was 0.192 in./sec, approximately three times greater.

The ablative rates measured between thermocouples two and three were 0.085 in./sec for MXBE-350, 0.073 in./sec for Haveg 41N, and 0.119 in./sec for WA-1. The results of the measured ablation rates are summarized in Table 5.

---

* California Computer Products, Anaheim, CA

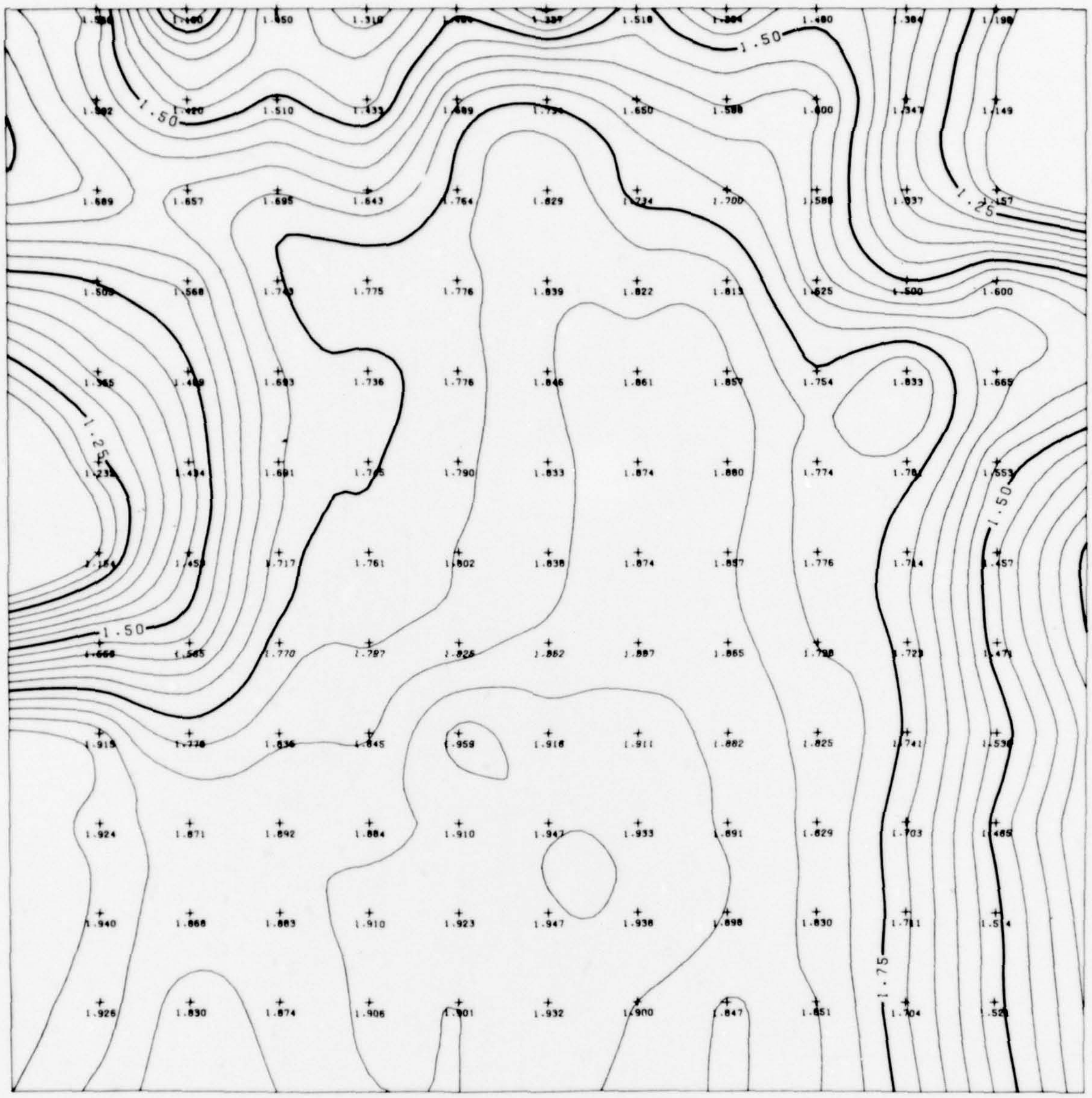

Figure 7. Haveg 41 Contours from Plenum A, Test 1, Motor L

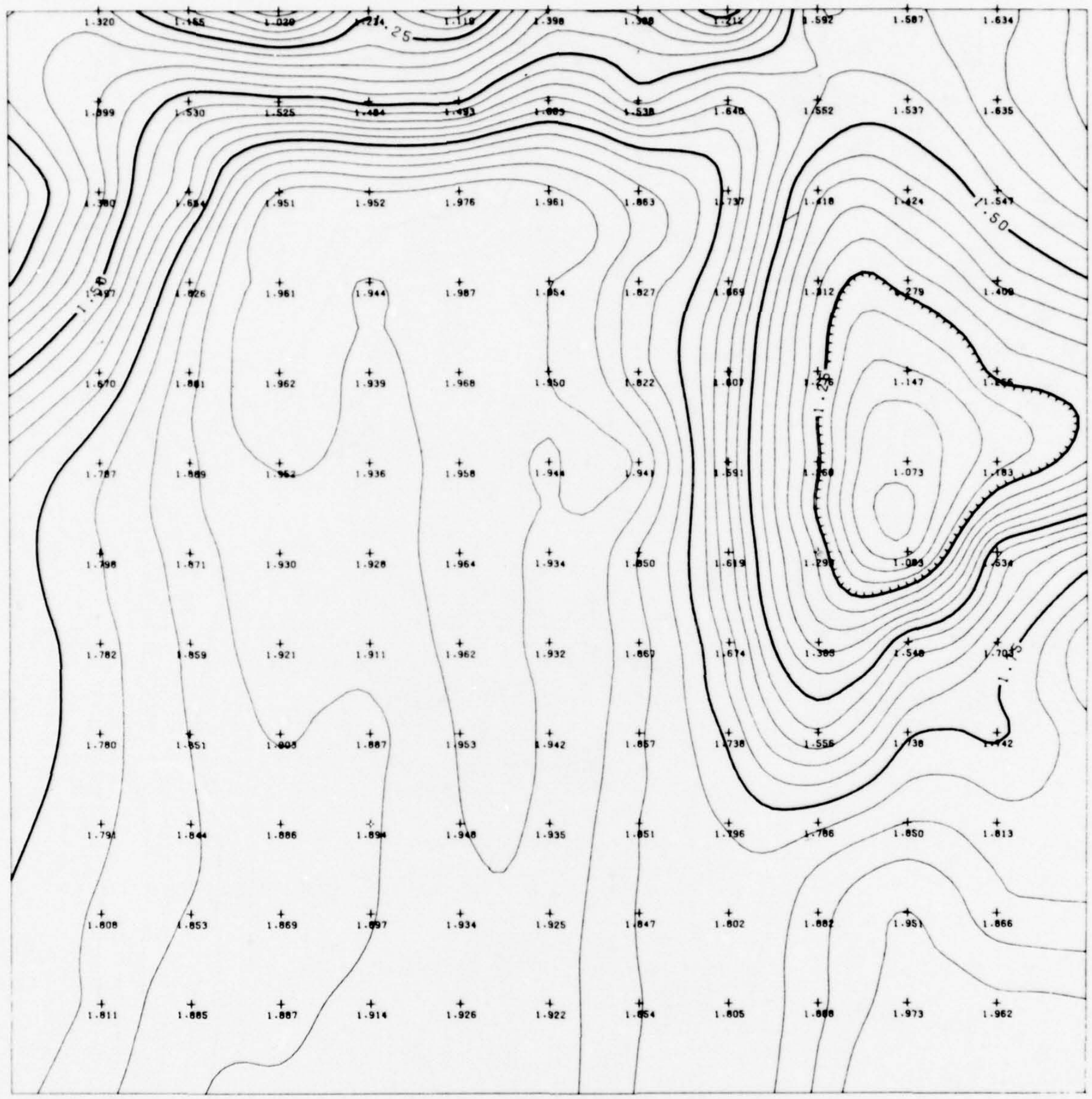

Figure 8. Haveg 41N Contours from Plenum A, Test 1, Motor R

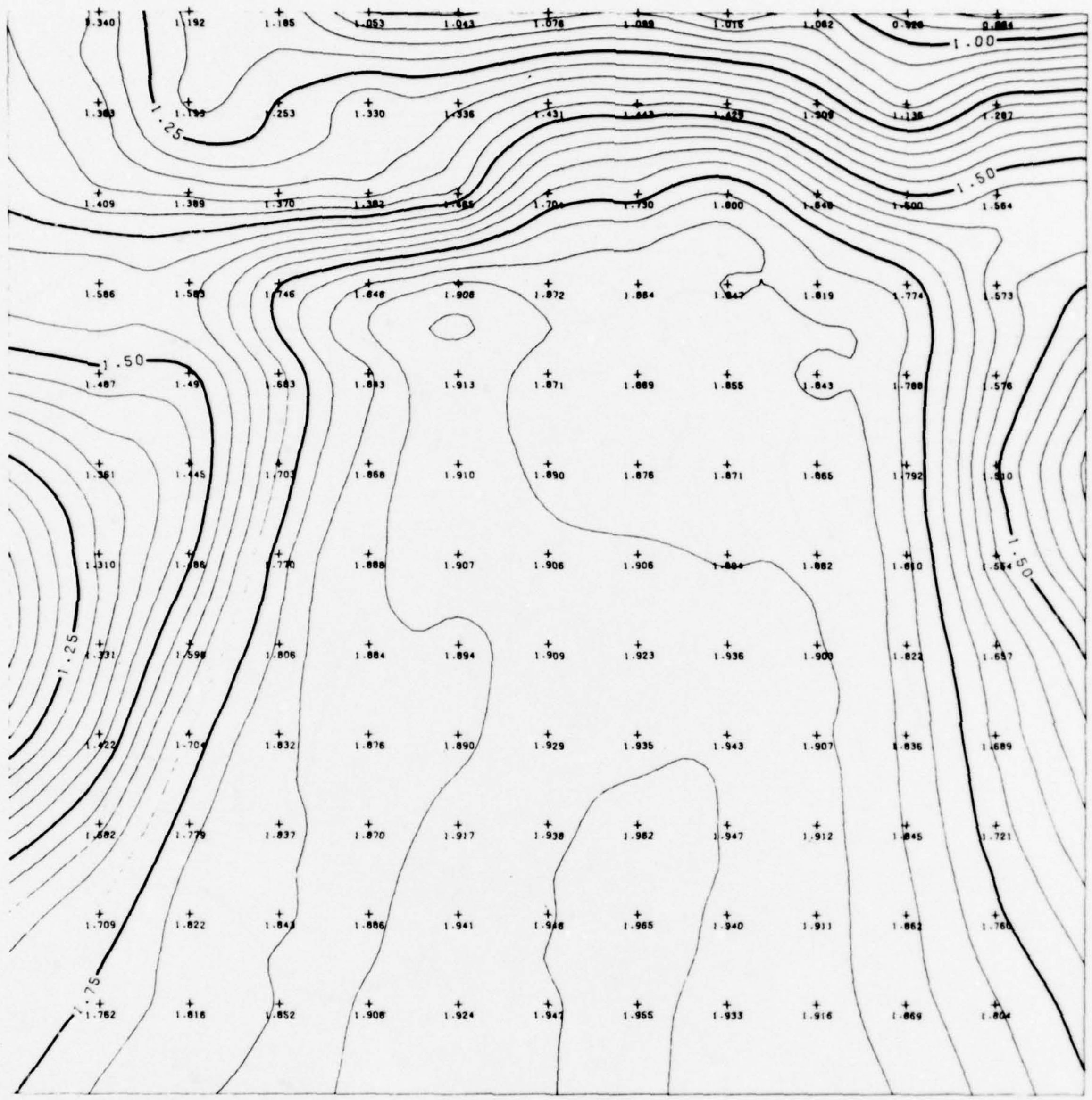

Figure 9. MXB-360 Contours from Plenum A, Test 2, Motor L

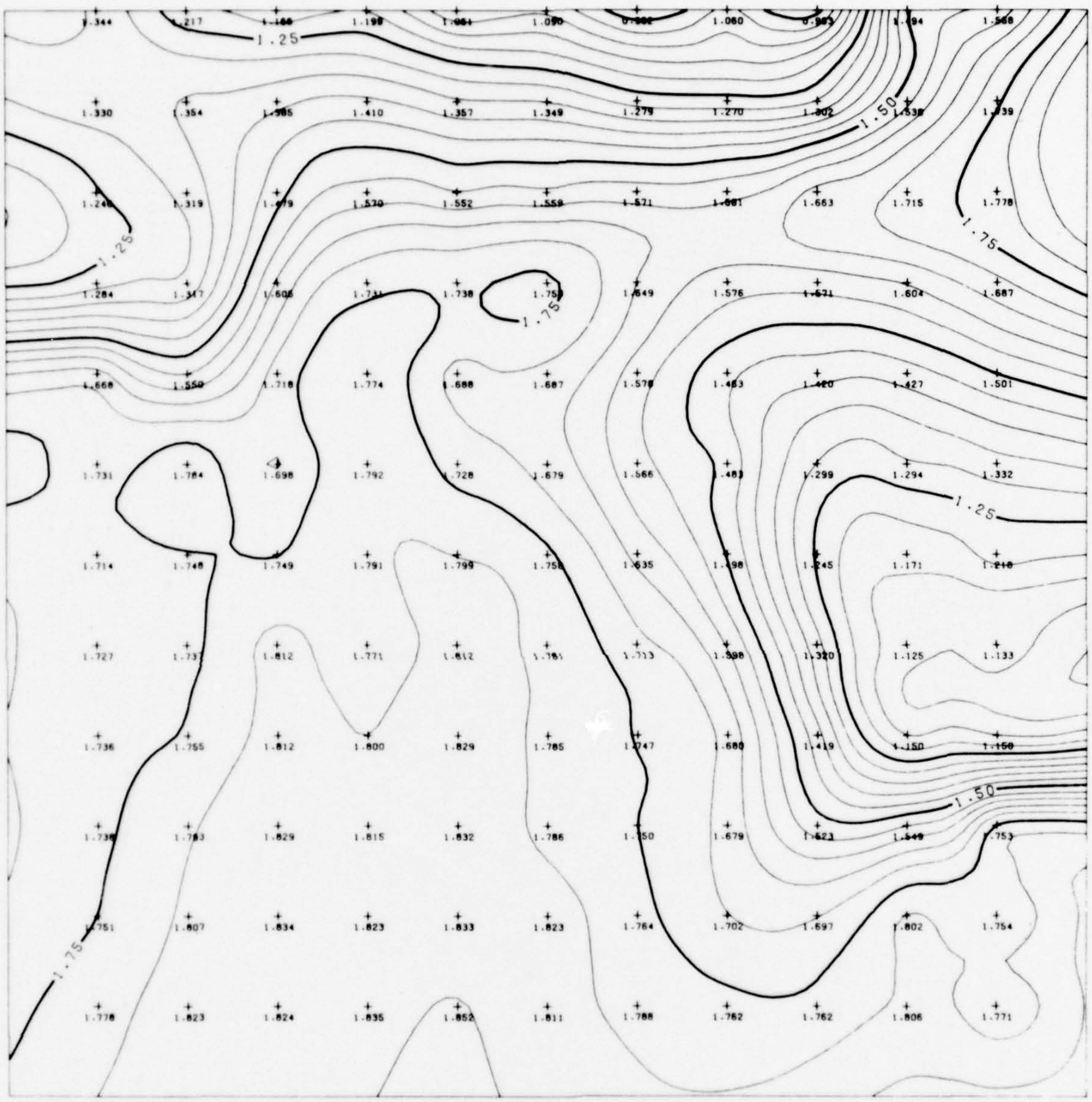

Figure 10. FR-1 Contours from Plenum A, Test 2, Motor R

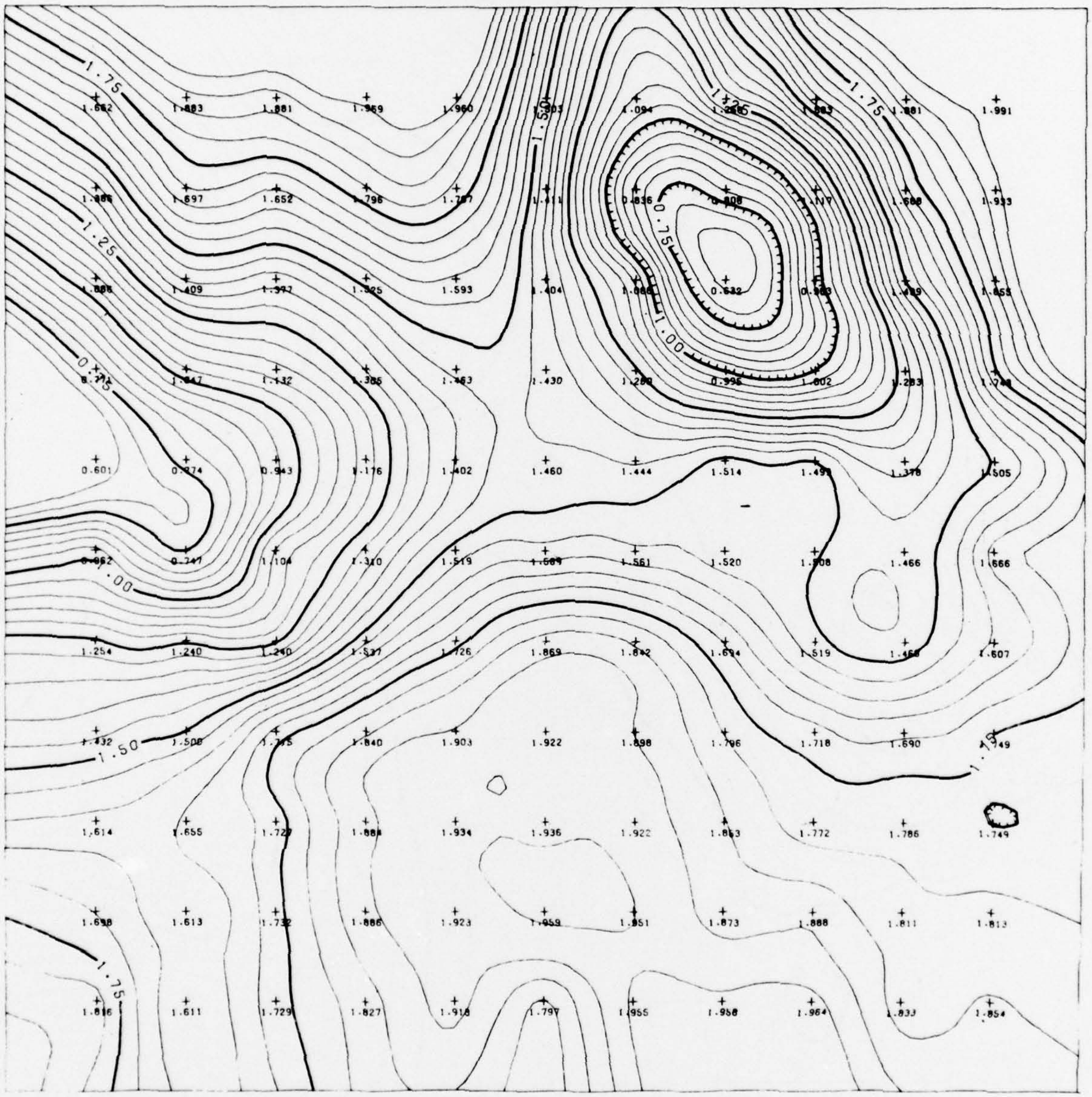

Figure 11. Haveg 41N Contours from Plenum B, Test 3, Motor L

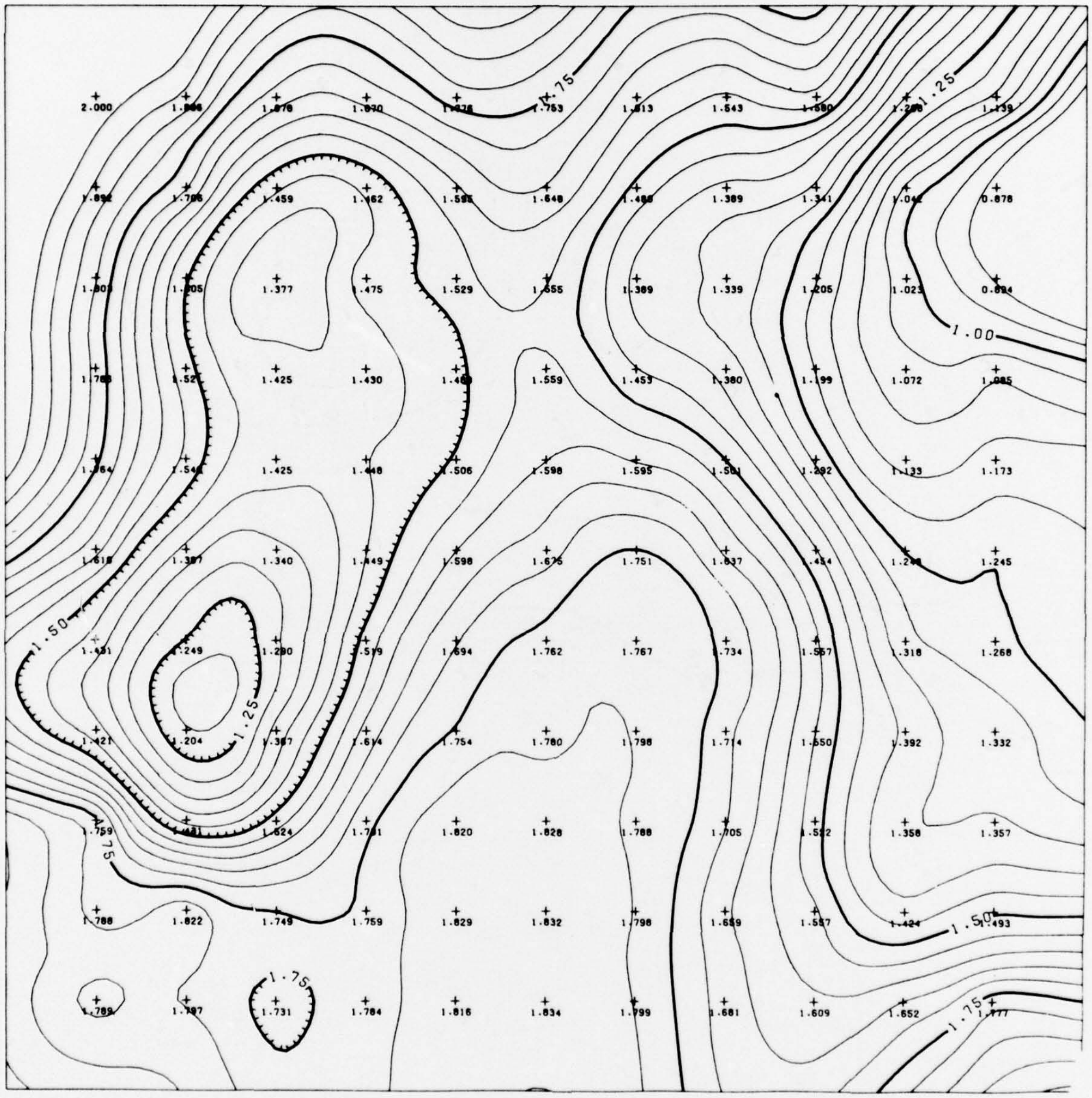

Figure 12. Haveg 41 Contours from Plenum B, Test 3, Motor R

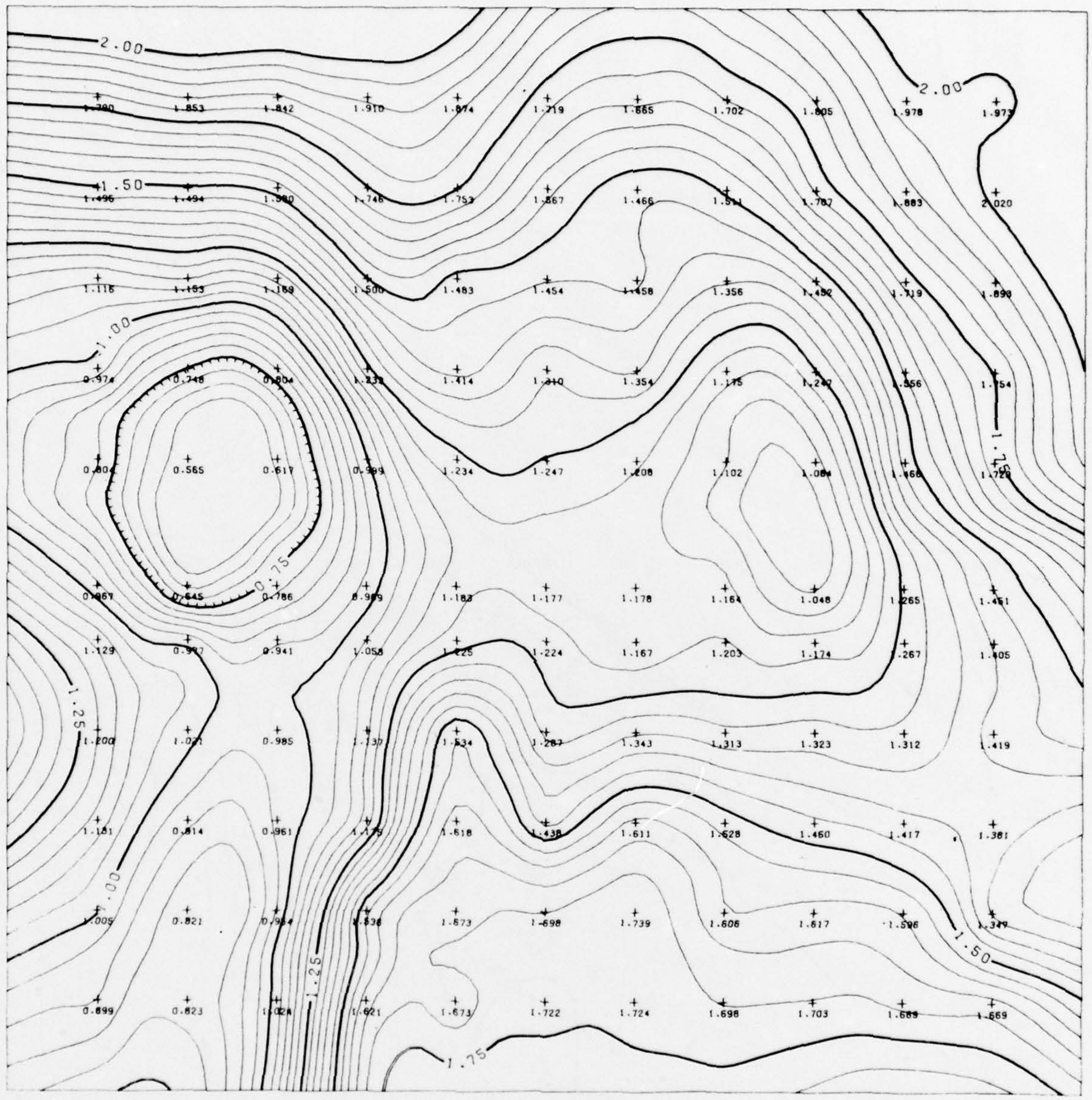

Figure 13. Fondu-Fyre WA-1 Contours from Plenum B, Test 4, Motor L

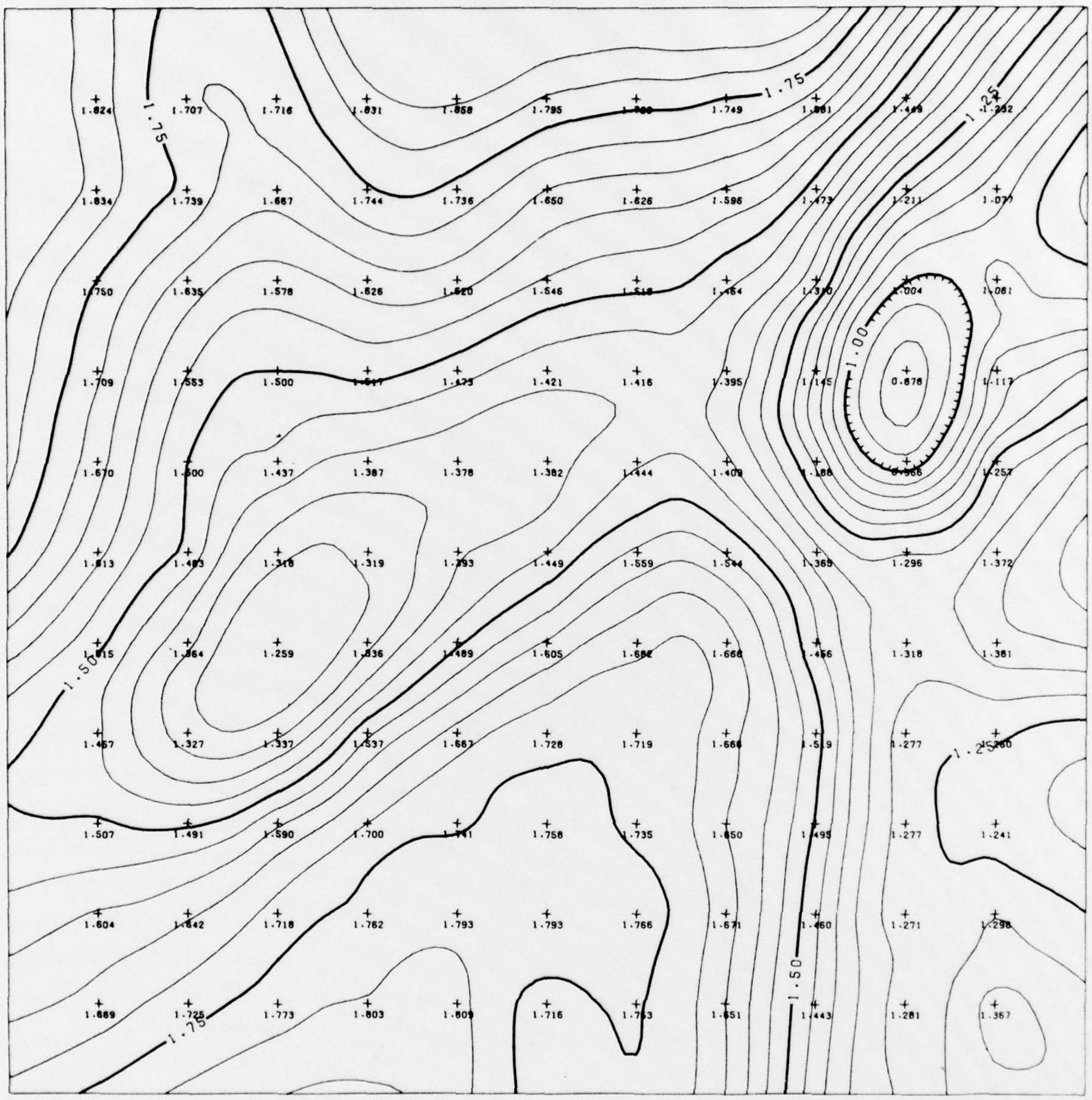

Figure 14. Haveg 41N Contours from Plenum B, Test 4, Motor R

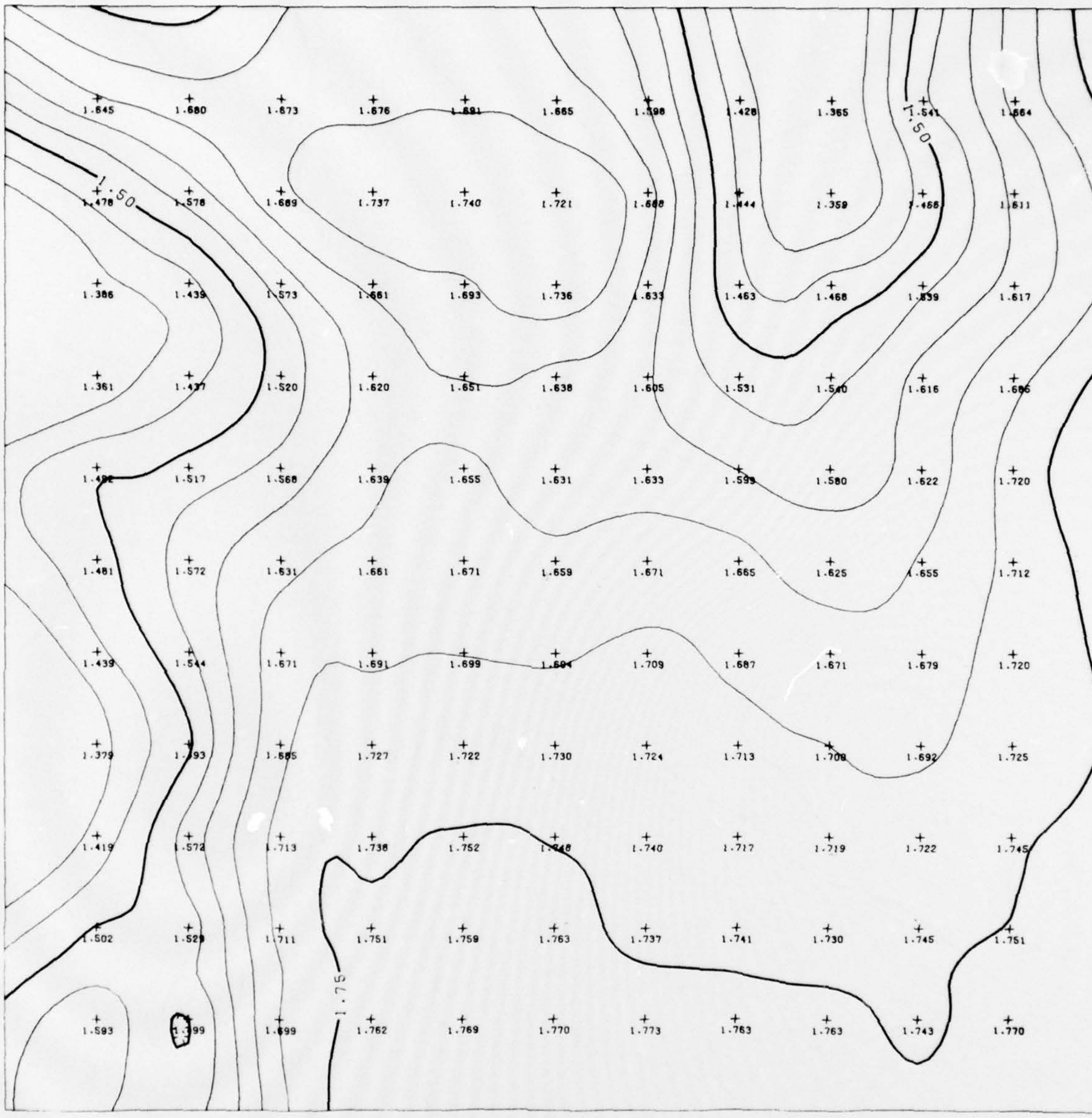

Figure 15. HDFG Carbon Contours from Plenum B, Test 5, Motor L

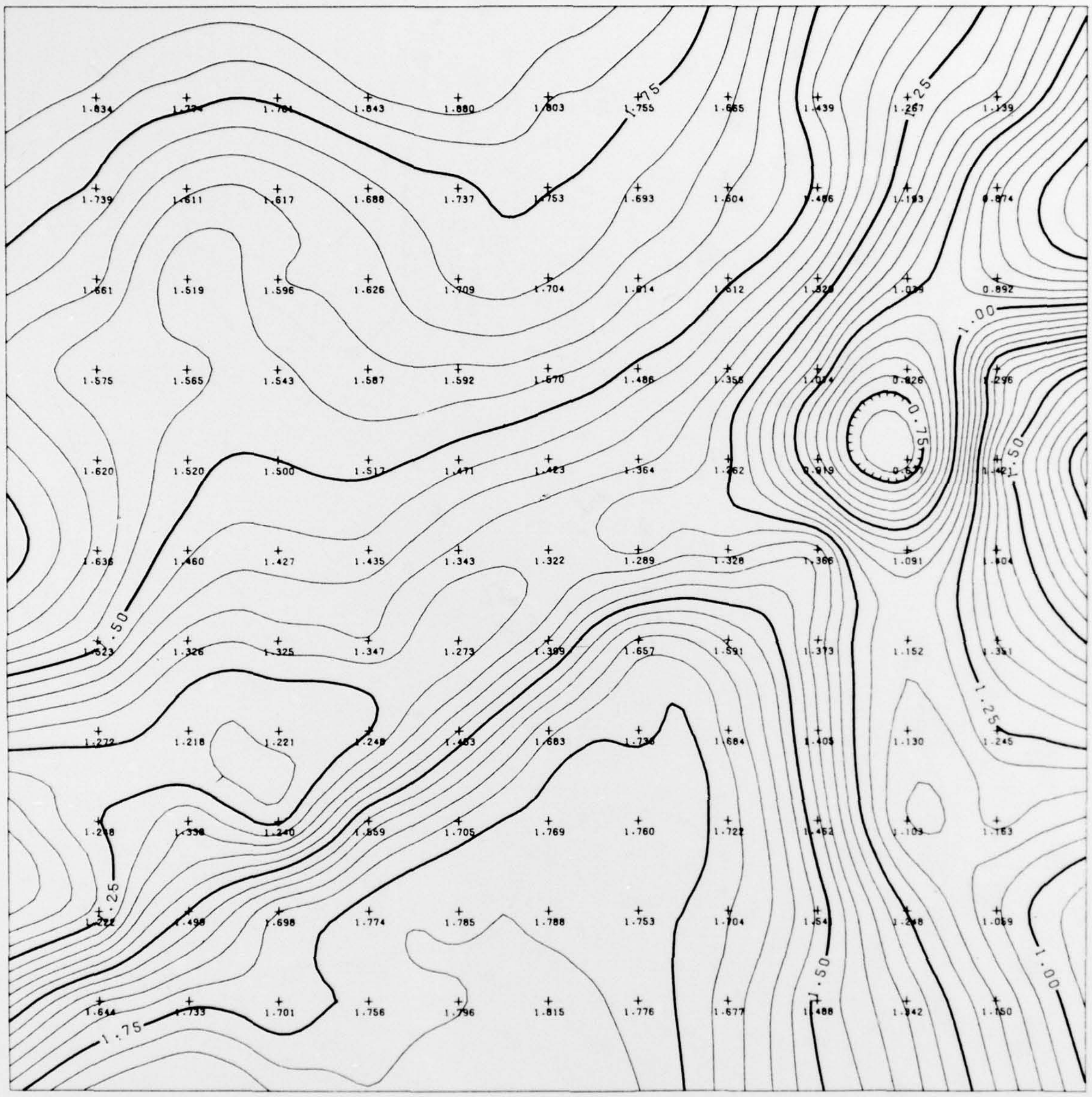

Figure 16. MXBE-350 Contours from Plenum B, Test 5, Motor R

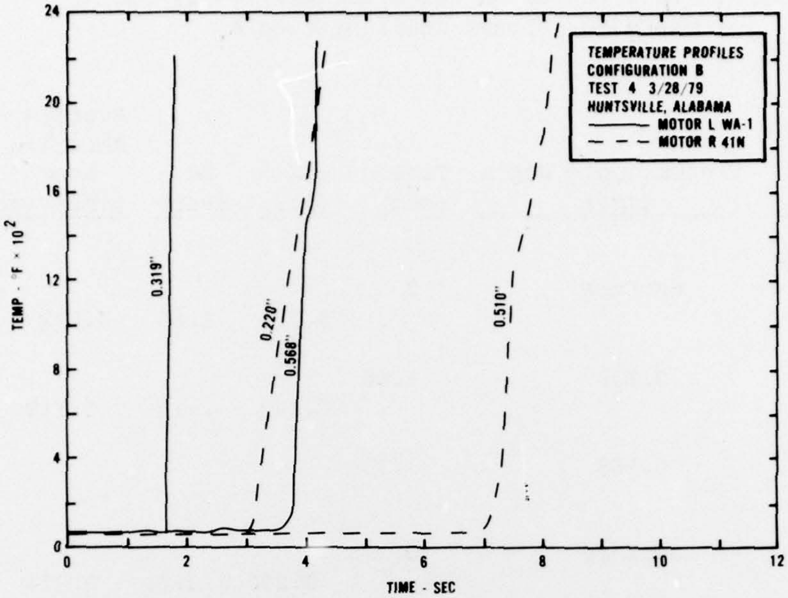

Figure 17. Temperature Profiles for Haveg 41N and Fondu-Fyre WA-1

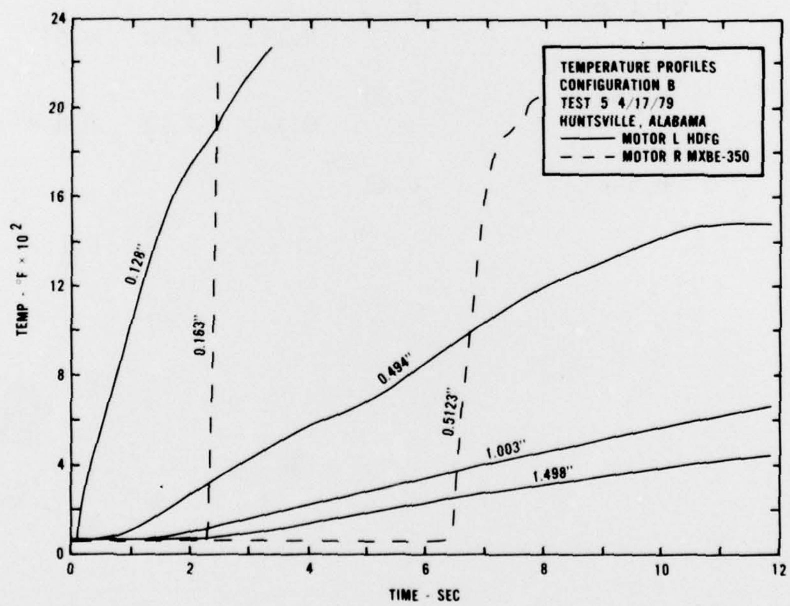

Figure 18. Temperature Profiles for HDFG and MXBE-350

Table 5. Local Ablation Rates for 41N, WA-1, and MXBE-350, Plenum Configuration B

Ablative Material	Thermocouple Depth (in.)	Time (sec)	ΔX (in.)	Δt (sec)	Average Ablation Rate (in./sec)
Fondu-Fyre WA-1	Surface	0			
			0.319	1.66	0.192
	0.319	1.66			
			0.249	2.10	0.119
	0.568	3.76			
41N	Surface	0			
			0.220	3.11	0.071
	0.220	3.11			
			0.290	4.00	0.073
	0.510	7.11			
MXBE-350	Surface	0			
			0.163	2.30	0.071
	0.163	2.30			
			0.349	4.12	0.085
	0.512	6.42			

CONCLUSIONS

Although the test conditions could not be controlled as accurately as desired, several useful comparisons and conclusions can be made from the results. HDFG carbon was the least eroded of the materials tested. Its mass loss and maximum erosion depth were less than one-third of the next best material tested. The HDFG is, however, a poor insulator and therefore may not be useful in areas where maximum thermal protection is required.

MXB-360, Haveg 41, Haveg 41N, and Fondu-Fyre WA-1 were approximately equal in maximum erosion depth and total mass loss (within 15 percent). MXBE-350 was slightly less effective. The FR-1 ablative compared equally well with the other charring materials where ranked by maximum erosion depth. However, FR-1 lost twice the total mass (percent) compared with Haveg 41N.

RECOMMENDATIONS

Although the results obtained in these tests were satisfactory, certain changes should be made before the next series of tests.

The thermocouples were positioned so that only the 0.125- and 0.50-in. depths experienced a temperature rise. In the next series of tests, five thermocouples should be located at 0.125-in. intervals to a depth of 0.625-in. With the closer spacing, more accurate temperature profile measurements and ablation rates will be possible.

In addition to relocation, the thermocouple type should be changed from chromel-alumel to tungsten-rhenium. This change will allow the measurements of material temperatures to be increased from a maximum of 2400°F to over 5000°F.

Heat flux transducers and radiometers should be used in the next series of tests to obtain the heat transfer to the surface of the material.

These changes will yield more accurate data, thus increasing the accuracy of the resulting calculations. The addition of the heat flux transducers will allow the calculation of ablation rates as a function of the heat flux for all the materials tested.

APPENDIX A

MOTOR DATA

APPENDIX A

MOTOR DATA

THIOKOL TOMAHAWK
MODEL TE-M-416

MOTOR PERFORMANCE*	
Burn Time**/Action Time, sec	8.31/8.85
Burn Time Avg. Cham. Press., psia	920
Action Time Avg. Cham. Press., psia	880
Maximum Chamber Pressure, psia	1,210
Total Impulse, lbf-sec	93,800
Burn Time Impulse, lbf-sec	91,100
Burn Time Average Thrust, lbf	11,000
Action Time Average Thrust, lbf	10,600
Maximum Thrust, lbf	15,000
NOZZLE	
Initial Throat Area, $in.^2$	8.56
Exit Area, $in.^2$	57.01
Expansion Ratio	6.66
Expansion Cone Half Angle, degrees	15
PROPELLANT	
Propellant Designation	TP-H-3095
Propellant Weight, lbm	387.06
Propellant Type	Aluminized Amonium Perchlorate
PROPELLANT CHARACTERISTICS	
Adiabatic Flame Temperature, °F	5,953
Effective Ratio of Specific Heats	1.16

* 60°F, Sea Level
** Determined by the two-tangent method

APPENDIX B

CHAMBER PRESSURE DATA

FOR TOMAHAWK TESTS

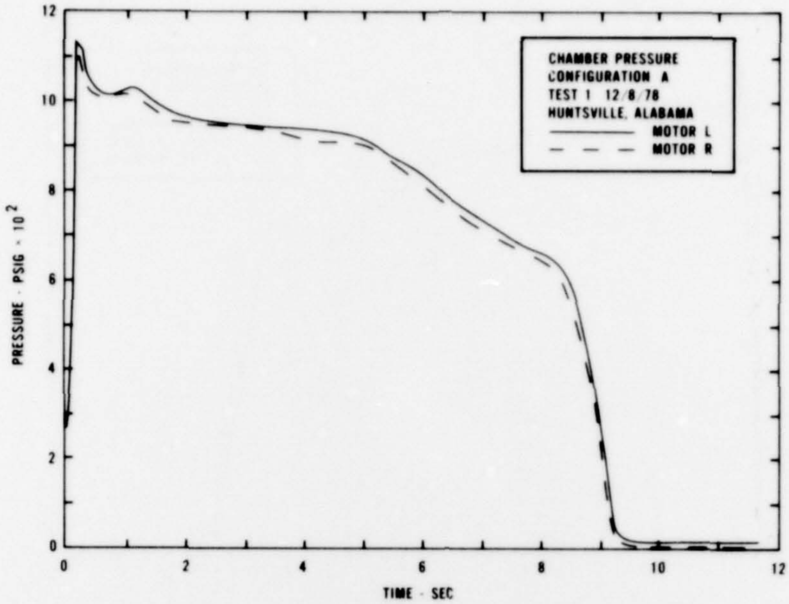

Figure B-1. Comparison of Chamber Pressures, Motors L and R, Plenum A, Test 1

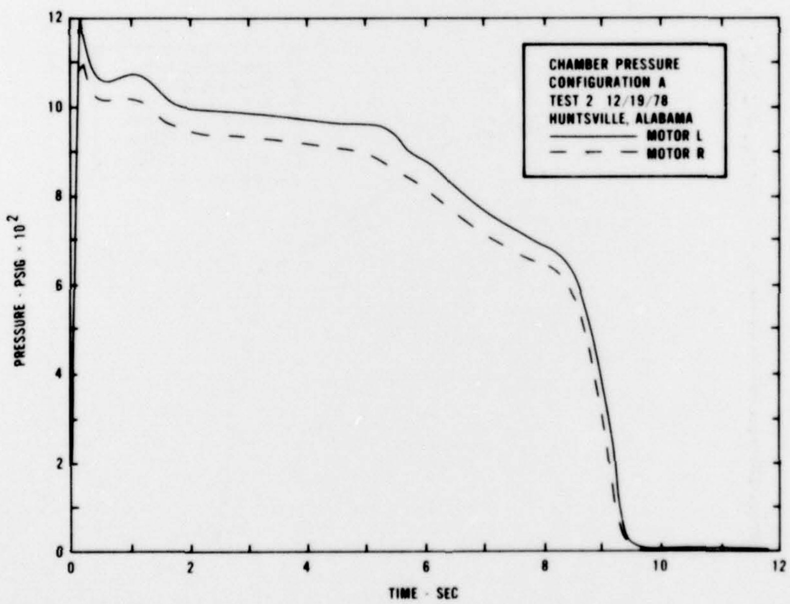

Figure B-2. Comparison of Chamber Pressures, Motors L and R, Plenum A, Test 2

PRECEDING PAGE NOT FILMED
BLANK

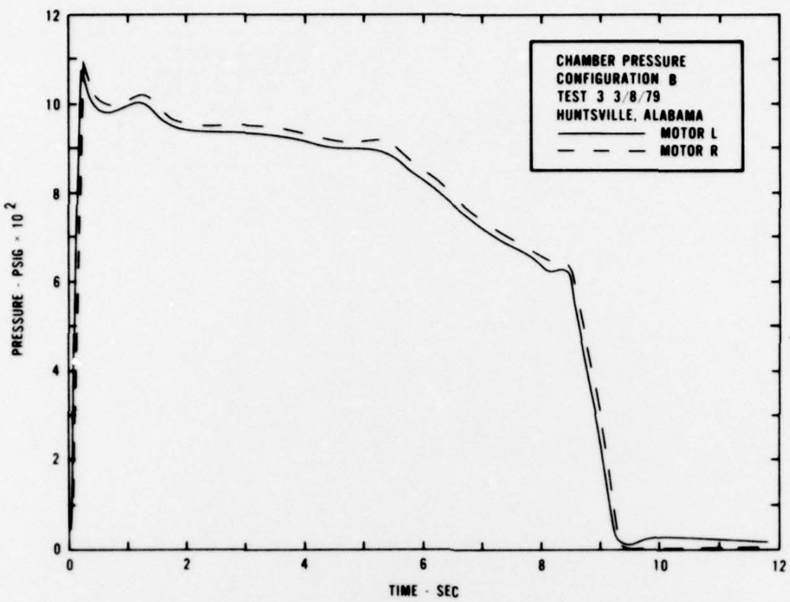

Figure B-3. Comparison of Chamber Pressures, Motors L and R, Plenum B, Test 3

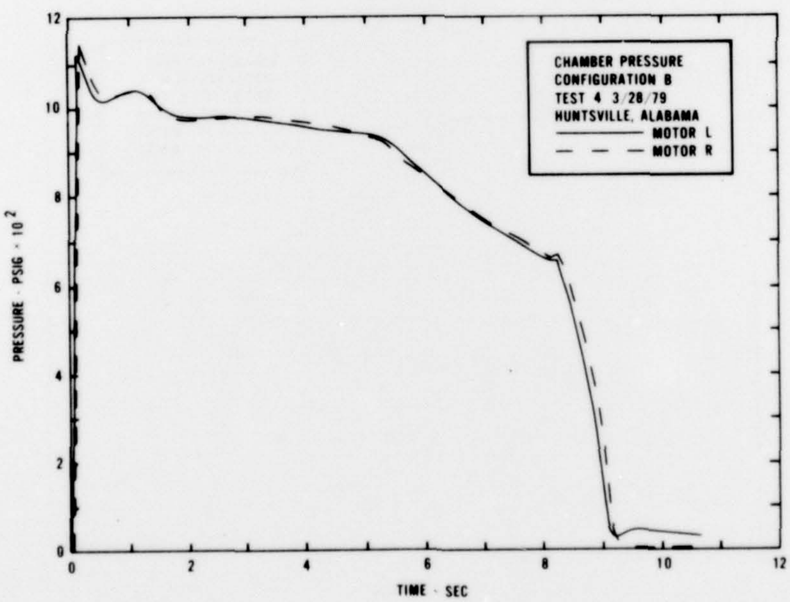

Figure B-4. Comparison of Chamber Pressures, Motors L and R, Plenum B, Test 4

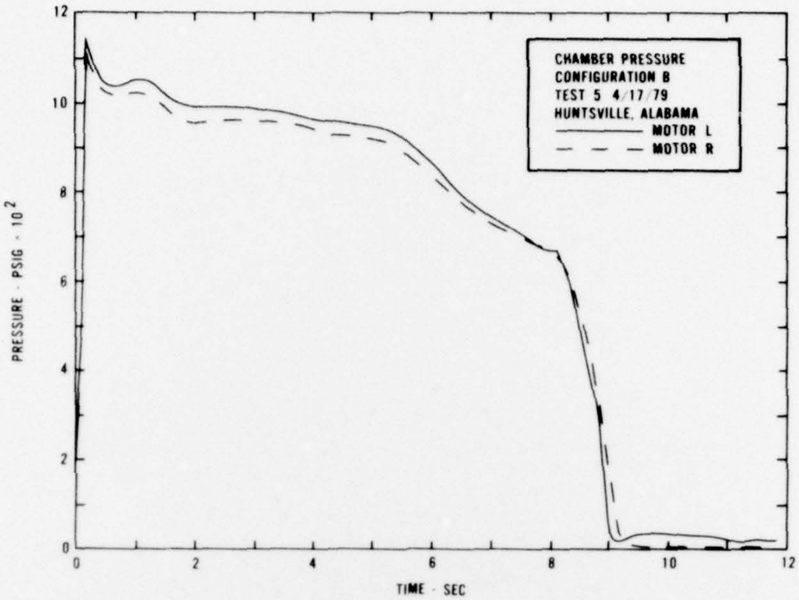

Figure B-5. Comparison of Chamber Pressures, Motors L and R, Plenum B, Test 5

DISTRIBUTION

Commander
Naval Sea System Command
Washington, DC 20362
ATTN: SEA-03513 (L. Pasiuk)

Commander
Naval Research Laboratory
Washington, DC 20390

Chief of Naval Research
Department of the Navy
Washington, DC 20390

Chief of Naval Operations
Department of the Navy
Washington, DC 20350

Chief of Naval Material
Department of the Navy
Washington, DC 23060

Director
Defense Nuclear Agency
Washington, DC 20305

Fiberite Corporation
Division of Universal Manufacturing Company
512 West 4th Street
Winona, MN 55987
ATTN: John Beard

Fiber Materials, Inc.
Biddeford Industrial Park
Biddeford, ME 04005
ATTN: Herb Dietrich

Chrysler Corporation
Department 2731
P. O. Box 29200
New Orleans, LA 70189
ATTN: Roger Keefe

Haveg Industries
Chemical Equipment Division
900 Greenbank Road
Wilmington, DE 19808
ATTN: Roy Wilde

DISTRIBUTION (Continued)

NASA Marshall Spaceflight Center Huntsville, AL 35812 ATTN: Bob Dunn	
Defense Documentation Center Cameron Station Alexandria, VA 22314	(12)
Library of Congress Washington, DC 20540 ATTN: Gift and Exchange Division	(4)

<u>Local:</u>

E41	
G	
G25 (Coates)	(4)
N	
N40	
N43	
N43 (Henderson)	(30)
X210	(2)
X211	(2)